Advection-diffusion on uncertain geometries

By M. Wahlsten†, J. Nordström† AND G. Iaccarino

The two-dimensional advection–diffusion equation on a stochastically varying geometry is considered. The varying domain is transformed into a fixed one and the numerical solution is computed using a high-order finite difference formulation on summation-by-parts form with weakly imposed boundary conditions. Statistics of the solution are computed non-intrusively using quadrature rules given by the probability density function of the random variable. As a quality control, we prove that the continuous problem is strongly well-posed, that the semi-discrete problem is strongly stable and verify the accuracy of the scheme. The technique is applied to a heat conduction problem in incompressible flow. The variance of the solution in terms of a functional is computed and discussed. We show that there is an increasing sensitivity to geometric uncertainty as we gradually increase the frequency and amplitude of the randomness.

1. Introduction

When solving partial differential equations, uncertain geometry of the computational domain may arise for many reasons. Examples include irregular materials, inaccurate CAD (Computer-Aided Design) software, imprecise manufacturing machines and imperfect mesh generators. We study the effects of this uncertainty and impose the boundary condition at stochastically varying positions in space. Other techniques dealing with geometric uncertainty include polynomial chaos with remeshing of geometry (Lin *et al.* 2008) as well as chaos collocation methods with fictious domains (Parussini *et al.* 2010).

The stochastically varying domain is transformed into a fixed one. This procedure has previously been used in Xiu & Tartakovsky (2006) for elliptic problems. The analysis is extended in this paper to the time-dependent advection–diffusion equation governing the temperature distribution in incompressible flow.

The continuous problem is analyzed using the energy method, and strong well-posedness is proved, [see Eliasson *et al.* (2009); Nordström *et al.* (2012); Nordström & Svärd (2005)]. We discretize using high-order finite difference methods on summation-by-parts form with weakly imposed boundary conditions, and prove strong stability, [see for instance Svärd & Nordström (2014*b*,*a*)]. The statistics of the solution such as the mean, variance and confidence intervals are computed non-intrusively using quadrature rules for the given stochastic distributions (Lin *et al.* 2010; Mendes *et al.* 2012). As an application, we analyze the heat conduction at rough surfaces in incompressible flow (Seban 2012; Antohe & Lage 1997; Patankar & Spalding 1972).

The paper will proceed as follows: In Section 2, we define the continuous problem in two space dimensions, transform it to the unit square using curvilinear coordinates and derive energy estimates that lead to well-posedness. We formulate a finite difference scheme for the continuous problem and prove stability in Section 3. In Section 4, we consider a heat conduction problem in incompressible flow. Finally, in Section 5 we draw conclusions.

† Linköping University, Sweden

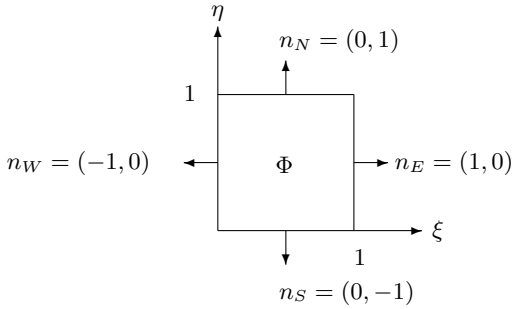

FIGURE 1: The transformed domain including normal vectors for the east, west, north and south boundaries (n_E, n_W, n_N and n_S).

2. The continuous problem

Consider the advection–diffusion problem on the stochastically varying domain $\Omega(\vec{\theta})$

$$\begin{array}{rcll} u_t + \bar{u}u_x + \bar{v}u_y &=& (\epsilon u_x)_x + (\epsilon u_y)_y + F(x,y,t), & (x,y) \in \Omega(\vec{\theta}), \quad t \geq 0 \\ Hu(x,y,t,\vec{\theta}) &=& g(x,y,t), & (x,y) \in \partial\Omega(\vec{\theta}), \quad t \geq 0 \\ u(x,y,0,\vec{\theta}) &=& f(x,y), & (x,y) \in \Omega(\vec{\theta}), \quad t = 0. \end{array} \tag{2.1}$$

In Eq. (2.1), $\bar{u}$ and $\bar{v}$ are the mean velocities in the $x-$ and $y-$directions, satisfying the divergence relation $\bar{u}_x + \bar{v}_y = 0$ stemming from an incompressible Navier–Stokes solution. Furthermore, $\epsilon = \epsilon(x,y,t)$ is a positive diffusion coefficient, $u = u(x,\, y,\, t,\, \vec{\theta})$ represents the solution to the problem and $\vec{\theta} = (\theta_1,\, \theta_2,\, \ldots)$ is a vector of random variables describing the geometry of the domain. F, g and f are data to the problem. The goal of this study is to investigate the effects of placing the boundary condition $Hu = g$ at the stochastically varying boundary $(x,\, y) \in \partial\Omega(\vec{\theta})$.

2.1. *The transformation*

We now transform the stochastically varying domain Ω into the unit square. By applying the chain rule to Eq. (2.1), multiplying by $J = x_\xi y_\eta - x_\eta y_\xi > 0$, using metric relations, the Geometric Conservation Law (GCL) (Farhat *et al.* 2001) and the divergence relation $\bar{u}_x + \bar{v}_y = 0$, we obtain

$$\begin{array}{rcll} Ju_t + (\tilde{a}u)_\xi + (\tilde{b}u)_\eta &=& \tilde{f}_\xi + \tilde{g}_\eta + JF(\xi,\eta,t), & (\xi,\eta) \in \Phi, \quad t \geq 0 \\ \tilde{H}u(\xi,\eta,t,\vec{\theta}) &=& g(\xi,\eta,t), & (\xi,\eta) \in \partial\Phi, \quad t \geq 0 \\ u(\xi,\eta,0,\vec{\theta}) &=& f(\xi,\eta), & (\xi,\eta) \in \Phi, \quad t = 0, \end{array} \tag{2.2}$$

where

$$\begin{array}{rclrcl} \tilde{a} &=& J[(\bar{u},\bar{v}) \cdot \nabla\xi] & \tilde{f} &=& J[\epsilon(\nabla u \cdot \nabla\xi)] \\ \tilde{b} &=& J[(\bar{u},\bar{v}) \cdot \nabla\eta] & \tilde{g} &=& J[\epsilon(\nabla u \cdot \nabla\eta)] \end{array} \tag{2.3}$$

and $\Phi = [0,\, 1] \times [0,\, 1]$. In Eq. (2.3), we have used the notation $\nabla = \left(\dfrac{\partial}{\partial x}, \dfrac{\partial}{\partial x}\right)^T$. The transformed fixed domain is presented in Figure 1. Note that the wave speeds $\tilde{a}$ and $\tilde{b}$ depend on the stochastic variables $\vec{\theta}$.

2.2. *The energy method*

To derive well-posed boundary conditions, we apply the energy method (multiply by the solution and integrate in space) on the transformed problem Eq. (2.2). This procedure

gives the following boundary conditions for the case $\tilde{a}, \tilde{b} \neq 0$

$$H_E^- u = g_E \quad H_W^- u = g_W \quad H_N^- u = g_N \quad H_S^- u = g_S, \tag{2.4}$$

where

$$\begin{aligned}
H_E^- &= \begin{cases} 1 - \frac{1}{\tilde{a}}\left(\tilde{D}_{11}\frac{\partial}{\partial\xi} + \tilde{D}_{12}\frac{\partial}{\partial\eta}\right) & \text{if } \tilde{a}\big|^{\xi=1} < 0 \\ \tilde{D}_{11}\frac{\partial}{\partial\xi} + \tilde{D}_{12}\frac{\partial}{\partial\eta} & \text{if } \tilde{a}\big|^{\xi=1} > 0 \end{cases} \\
H_W^- &= \begin{cases} 1 - \frac{1}{\tilde{a}}\left(\tilde{D}_{11}\frac{\partial}{\partial\xi} + \tilde{D}_{12}\frac{\partial}{\partial\eta}\right) & \text{if } \tilde{a}\big|_{\xi=0} > 0 \\ \tilde{D}_{11}\frac{\partial}{\partial\xi} + \tilde{D}_{12}\frac{\partial}{\partial\eta} & \text{if } \tilde{a}\big|_{\xi=0} < 0 \end{cases} \\
H_N^- &= \begin{cases} 1 - \frac{1}{\tilde{b}}\left(\tilde{D}_{21}\frac{\partial}{\partial\xi} + \tilde{D}_{22}\frac{\partial}{\partial\eta}\right) & \text{if } \tilde{b}\big|^{\eta=1} < 0 \\ \tilde{D}_{21}\frac{\partial}{\partial\xi} + \tilde{D}_{22}\frac{\partial}{\partial\eta} & \text{if } \tilde{b}\big|^{\eta=1} > 0 \end{cases} \\
H_S^- &= \begin{cases} 1 - \frac{1}{\tilde{b}}\left(\tilde{D}_{21}\frac{\partial}{\partial\xi} + \tilde{D}_{22}\frac{\partial}{\partial\eta}\right) & \text{if } \tilde{b}\big|_{\eta=0} > 0 \\ \tilde{D}_{21}\frac{\partial}{\partial\xi} + \tilde{D}_{22}\frac{\partial}{\partial\eta} & \text{if } \tilde{b}\big|_{\eta=0} < 0. \end{cases}
\end{aligned} \tag{2.5}$$

The boundary operators in Eq. (2.5) yield a well-posed problem.

2.3. *Weak imposition of boundary conditions*

As a preparation for the numerical approximation, we now impose the boundary conditions weakly. This gives

$$\begin{aligned}
\frac{d}{dt}\|u\|_J^2 + 2DI = &- \int_0^1 \tilde{a}u^2 - 2u\tilde{f}\Big|_{\xi=0}^{\xi=1} d\eta - \int_0^1 \tilde{b}u^2 - 2u\tilde{g}\Big|_{\eta=0}^{\eta=1} d\xi \\
&+ 2\int_0^1 u\Sigma_E(W_E^- - g_E)\Big|^{\xi=1} + u\Sigma_W(W_W^- - g_W)\Big|_{\xi=0} d\eta \\
&+ 2\int_0^1 u\Sigma_N(W_N^- - g_N)\Big|^{\eta=1} + u\Sigma_S(W_S^- - g_S)\Big|_{\eta=0} d\xi
\end{aligned} \tag{2.6}$$

where $DI = \int_\Omega \epsilon J|\nabla u|^2\, dx\, dy$.

Proposition 1. *The problem Eq. (2.2) with the boundary conditions Eq. (2.4) and the penalty coefficients*

$$\begin{aligned}
\Sigma_E &= \begin{cases} -\tilde{a} & \text{if } \tilde{a} < 0 \\ -1 & \text{if } \tilde{a} > 0 \end{cases} \qquad \Sigma_W = \begin{cases} -\tilde{a} & \text{if } \tilde{a} > 0 \\ -1 & \text{if } \tilde{a} < 0 \end{cases} \\
\Sigma_N &= \begin{cases} -\tilde{b} & \text{if } \tilde{b} < 0 \\ -1 & \text{if } \tilde{b} > 0 \end{cases} \qquad \Sigma_S = \begin{cases} -\tilde{b} & \text{if } \tilde{b} > 0 \\ -1 & \text{if } \tilde{b} < 0 \end{cases}
\end{aligned} \tag{2.7}$$

is strongly well-posed.

We perform the proof for the specific case $\tilde{a}, \tilde{b} > 0$. For other values of $\tilde{a}$ and $\tilde{b}$, exactly the same procedure is used. The energy method is applied to Eq. (2.1) with the penalty

parameters in Eq. (2.7) together with an integration in time (from 0 to T) results in

$$\begin{aligned}
\|u(T)\|_J^2 + 2\int_0^T DI\,dt &= \|f\|_J^2 \\
&- \int_0^T \int_0^1 \tilde{a}\left(u - \frac{g_E}{\tilde{a}}\right)^2 - \frac{g_E^2}{\tilde{a}}\Big|^{\xi=1} d\eta\,dt \\
&- \int_0^T \int_0^1 \tilde{a}(u-g_W)^2 - g_W^2\tilde{a}\Big|_{\xi=0} d\eta\,dt \\
&- \int_0^T \int_0^1 \tilde{b}\left(u - \frac{g_N}{\tilde{b}}\right)^2 - \frac{g_N^2}{\tilde{b}}\Big|^{\eta=1} d\xi\,dt \\
&- \int_0^T \int_0^1 \tilde{b}(u-g_S)^2 - g_S^2\tilde{b}\Big|_{\eta=0} d\xi\,dt.
\end{aligned} \tag{2.8}$$

In Eq. (2.8), the boundary terms with zero data all give a non-positive contribution, and hence the solution is bounded by data. The bound leads directly to uniqueness, and existence is guaranteed by the fact that we use the correct (i.e., minimal) number of boundary conditions.

3. The semi-discrete formulation

In this section we consider the numerical approximation of Eq. (2.2) formulated by using Summation-By-Parts (SBP) operators with Simultaneous Approximation Terms (SAT), the so-called SBP-SAT technique (Svärd & Nordström 2014*b*). First, we rewrite our variable coefficient continuous problem Eq. (2.2), using the splitting technique described in Nordström (2006), to obtain

$$Ju_t + \frac{1}{2}[(\tilde{a}u)_\xi + \tilde{a}u_\xi + \tilde{a}_\xi u + (\tilde{b}u)_\eta + \tilde{b}u_\eta + \tilde{b}_\eta u] = \tilde{f}_\xi + \tilde{g}_\eta. \tag{3.1}$$

The corresponding semi-discrete version of Eq. (3.1) including penalty terms for the boundary conditions is

$$\begin{aligned}
\tilde{J}U_t &= \frac{1}{2}[(D_\xi\tilde{A}U + \tilde{A}D_\xi U + \tilde{A}_\xi U + D_\eta\tilde{B}U + \tilde{B}D_\eta U + \tilde{B}_\eta U] \\
&- D_\xi\tilde{F}_\xi - D_\eta\tilde{G}_\eta \\
&= (P_\xi^{-1}E_{NN}\otimes I_\eta)\mathbf{\Sigma_E}(\mathbf{H_E^-}U - g) \\
&+ (P_\xi^{-1}E_{0N}\otimes I_\eta)\mathbf{\Sigma_W}(\mathbf{H_W^-}U - g) \\
&+ (I_\xi\otimes P_\eta^{-1}E_{MM})\mathbf{\Sigma_N}(\mathbf{H_N^-}U - g) \\
&+ (I_\xi\otimes P_\eta^{-1}E_{0M})\mathbf{\Sigma_S}(\mathbf{H_S^-}U - g) \\
U(0) &= f
\end{aligned} \tag{3.2}$$

where

$$\begin{aligned}
D_\xi &= (P_\xi^{-1}Q_\xi\otimes I_\eta) & D_\eta &= (I_\xi\otimes P_\eta^{-1}Q_\eta) \\
\tilde{F} &= \mathbf{\tilde{D}_{11}}D_\xi U + \mathbf{\tilde{D}_{12}}D_\eta U & \tilde{G} &= \mathbf{\tilde{D}_{21}}D_\xi U + \mathbf{\tilde{D}_{22}}D_\eta U \\
\mathbf{\tilde{D}_{11}} &= \tilde{\epsilon}\tilde{J}(\tilde{\xi}_x^2 + \tilde{\xi}_y^2), & \mathbf{\tilde{D}_{12}} &= \tilde{\epsilon}\tilde{J}(\tilde{\eta}_x\tilde{\xi}_x + \tilde{\eta}_y\tilde{\xi}_y) \\
\mathbf{\tilde{D}_{21}} &= \tilde{\epsilon}\tilde{J}(\tilde{\xi}_x\tilde{\eta}_x + \tilde{\xi}_y\tilde{\eta}_y), & \mathbf{\tilde{D}_{22}} &= \tilde{\epsilon}\tilde{J}(\tilde{\eta}_x^2 + \tilde{\eta}_y^2).
\end{aligned} \tag{3.3}$$

In Eqs. (3.2)-(3.3), $P_{\xi,\eta}^{-1}Q_{\xi,\eta}$ are the finite difference operators, $P_{\xi,\eta}$ are diagonal positive definite matrices, and $Q_{\xi,\eta}$ are almost skew-symmetric matrices satisfying $Q_{\xi,\eta} + Q_{\xi,\eta}^T = B = diag[-1, 0, \ldots, 0, 1]$.

U is a vector containing the numerical solution $U_{i,j}$ which approximates $u(\xi_i, \eta_j)$ ordered as

$$U = \begin{bmatrix} U_0 \\ U_1 \\ \vdots \\ U_N \end{bmatrix}, \quad U_i = \begin{bmatrix} U_{i,0} \\ U_{i,1} \\ \vdots \\ U_{i,M} \end{bmatrix}. \tag{3.4}$$

The indices $i = 0, 1, \ldots, N$ and $j = 0, 1, \ldots, M$ correspond to the grid points in ξ- and η-direction.

To ease the notation we denote $(P_\xi^{-1} Q_\xi \otimes I_\eta)U = U_\xi$ and $(I_\xi \otimes P_\eta^{-1} Q_\eta)U = U_\eta$ as the discrete derivatives with respect to ξ and η. E_{0N} and E_{0M} are zero matrices with the exception of the first element which is equal to one, and the corresponding sizes of the matrices are $(N+1) \times (N+1)$ and $(M+1) \times (M+1)$. Similarly, E_{NN} and E_{MM} are zero matrices with the exception of the last element which is equal to one, and the corresponding sizes of the matrices are $(N+1) \times (N+1)$ and $(M+1) \times (M+1)$. The notations I_ξ, I_η and $I_{\xi\eta}$ correspond to the identity matrices of sizes $(N+1) \times (N+1)$, $(M+1) \times (M+1)$ and $(M+1)(N+1) \times (M+1)(N+1)$, respectively. $\tilde{A}$, $\tilde{B}$, $\tilde{F}$, $\tilde{G}$, $\tilde{\xi}_x$, $\tilde{\xi}_y$, $\tilde{\eta}_x$, $\tilde{\eta}_y$, $\tilde{\epsilon}$ and $\tilde{J}$ are diagonal matrices approximating $\tilde{a}$, $\tilde{b}$, $\tilde{f}$, $\tilde{g}$, ξ_x, ξ_y, η_x, η_y, ϵ and J pointwise. The penalty matrices $\mathbf{\Sigma_E}, \mathbf{\Sigma_W}, \mathbf{\Sigma_N}$ and $\mathbf{\Sigma_S}$ will be chosen such that the numerical scheme Eq. (3.2) becomes stable.

The discrete boundary operators $\mathbf{H_E^-}$, $\mathbf{H_W^+}$, $\mathbf{H_N^-}$ and $\mathbf{H_S^+}$ are defined as

$$\begin{aligned}
\mathbf{H_E^-} &= \begin{cases} I_{\xi\eta} - \tilde{A}^{-1}\left(\tilde{\mathbf{D}}_{\mathbf{11}} D_\xi + \tilde{\mathbf{D}}_{\mathbf{12}} D_\eta\right) & \text{if } \tilde{A}\big|^{\xi=1} < 0 \\ \tilde{\mathbf{D}}_{\mathbf{11}} D_\xi + \tilde{\mathbf{D}}_{\mathbf{12}} D_\eta & \text{if } \tilde{A}\big|^{\xi=1} > 0 \end{cases} \\
\mathbf{H_W^-} &= \begin{cases} I_{\xi\eta} - \tilde{A}^{-1}\left(\tilde{\mathbf{D}}_{\mathbf{11}} D_\xi + \tilde{\mathbf{D}}_{\mathbf{12}} D_\eta\right) & \text{if } \tilde{A}\big|_{\xi=0} > 0 \\ \tilde{\mathbf{D}}_{\mathbf{11}} D_\xi + \tilde{\mathbf{D}}_{\mathbf{12}} D_\eta & \text{if } \tilde{A}\big|_{\xi=0} < 0 \end{cases} \\
\mathbf{H_N^-} &= \begin{cases} I_{\xi\eta} - \tilde{B}^{-1}\left(\tilde{\mathbf{D}}_{\mathbf{21}} D_\xi + \tilde{\mathbf{D}}_{\mathbf{22}} D_\eta\right) & \text{if } \tilde{B}\big|^{\eta=1} < 0 \\ \tilde{\mathbf{D}}_{\mathbf{21}} D_\xi + \tilde{\mathbf{D}}_{\mathbf{22}} D_\eta & \text{if } \tilde{B}\big|^{\eta=1} > 0 \end{cases} \\
\mathbf{H_S^-} &= \begin{cases} I_{\xi\eta} - \tilde{B}^{-1}\left(\tilde{\mathbf{D}}_{\mathbf{21}} D_\xi + \tilde{\mathbf{D}}_{\mathbf{22}} D_\eta\right) & \text{if } \tilde{B}\big|_{\eta=0} > 0 \\ \tilde{\mathbf{D}}_{\mathbf{21}} D_\xi + \tilde{\mathbf{D}}_{\mathbf{22}} D_\eta & \text{if } \tilde{B}\big|_{\eta=0} < 0 \end{cases}
\end{aligned} \tag{3.5}$$

which corresponds to the continuous counterparts in Eq. (2.5). (For more details on the SBP-SAT techniques, see Svärd & Nordström (2014*b*).)

3.1. *Stability*

Regarding stability of the numerical formulation Eq. (3.2) we rely on the following proposition:

Proposition 2. *The numerical approximation Eq. (3.2) using the penalty coefficients*

$$\begin{aligned}
\mathbf{\Sigma_E} &= \begin{cases} -\tilde{A} & \text{if } \tilde{a} < 0 \\ -I_{\xi\eta} & \text{if } \tilde{a} > 0 \end{cases} \qquad \mathbf{\Sigma_W} = \begin{cases} -\tilde{A} & \text{if } \tilde{a} > 0 \\ -I_{\xi\eta} & \text{if } \tilde{a} < 0 \end{cases} \\
\mathbf{\Sigma_N} &= \begin{cases} -\tilde{B} & \text{if } \tilde{b} < 0 \\ -I_{\xi\eta} & \text{if } \tilde{b} > 0 \end{cases} \qquad \mathbf{\Sigma_S} = \begin{cases} -\tilde{B} & \text{if } \tilde{b} > 0 \\ -I_{\xi\eta} & \text{if } \tilde{b} < 0 \end{cases}
\end{aligned} \tag{3.6}$$

is strongly stable.

For ease of presentation, we prove the special case when $\tilde{a}, \tilde{b} > 0$. By applying the discrete energy method on Eq. (3.2), using the parameters in Eq. (3.6) in time, eventually gives

$$\begin{aligned}
\|U(T)\|^2_{J(P_\xi \otimes P_\eta)} &+ 2\int_0^T \overline{DI}\, dt = \|f\|^2_{J(P_\xi \otimes P_\eta)} \\
&+ \int_0^T g^T (E_{NN} \otimes P_\eta)\tilde{A}^{-1} g + g^T (E_{0N} \otimes P_\eta)\tilde{A} g\, dt \\
&+ \int_0^T g^T (P_\xi \otimes E_{MM})\tilde{B}^{-1} g + g^T (P_\xi \otimes E_{0M})\tilde{B} g\, dt \\
&- \int_0^T (U - \tilde{A}^{-1} g)^T \tilde{A} (E_{NN} \otimes P_\eta)(U - \tilde{A}^{-1} g)\, dt \\
&- \int_0^T (U - g)^T \tilde{A} (E_{0N} \otimes P_\eta)(U - g)\, dt \\
&- \int_0^T (U - \tilde{B}^{-1} g)^T \tilde{B} (P_\xi \otimes E_{MM})(U - \tilde{B}^{-1} g)\, dt \\
&- \int_0^T (U - g)^T \tilde{B} (P_\xi \otimes E_{0M})(U - g)\, dt.
\end{aligned} \tag{3.7}$$

As in the continuous energy estimate Eq. (2.8), the RHS of Eq. (3.7) consists of boundary data and negative semi-definite dissipative boundary terms which result in a strongly stable numerical approximation.

Remark 1. *Note the similarity between the discrete energy estimate Eq. (3.7) and its continuous counterpart Eq. (2.8).*

4. Numerical results

We will compute various statistics for the given model problem Eq. (2.1) using the parameters $\bar{u} = \sin(x)\cos(y)$, $\bar{v} = -\cos(x)\sin(y)$, $\epsilon = 0.01$. We start with a quality control by using the method of manufactured solution (Roache 2002; Nordström & Wahlsten 2015) to verify the accuracy and stability of the scheme.

4.1. *Rate of convergence for the deterministic case*

The rate of convergence is verified by computing the order of accuracy p defined as

$$p = \log_2 \left(\frac{\|u_a - u_h\|_P}{\|u_a - u_{h/2}\|_P} \right). \tag{4.1}$$

In Eq. (4.1), u_h is the numerical solution, using the grid spacing h, and the manufactured solution is $u_a = \sin(2\pi(x-t)) + \sin(2\pi(y-t))$.

The order of accuracy computed for different number of grid points and SBP-operators, is shown in Table 1. As time-integrator, the classical 4th-order Runge-Kutta method with 5000 grid points was used. The results shown in Table 1 confirm that the scheme is accurate for the 2nd-, 3rd-, 4th- and 5th-order SBP-SAT schemes (Svärd & Nordström 2014*a*).

SBP operator/(N_x, N_y)	(20, 20)	(30, 30)	(40, 40)	(50, 50)
2nd order	1.979	1.989	1.993	1.996
3rd order	3.006	2.919	3.000	3.133
4th order	4.209	4.272	4.307	4.340
5th order	4.858	4.811	4.784	4.767

TABLE 1: The order of accuracy for the 2nd-, 3rd-, 4th- and 5th-order SBP-SAT schemes for different number of grid points in space.

4.2. *Heat conduction at rough surfaces*

Equipped with a provably stable scheme, we will now investigate the stochastic properties of a heat distribution problem in incompressible flow. The problem in two dimensions is of the form

$$T_t + \bar{u}T_x + \bar{v}T_y = (\epsilon T_x)_x + (\epsilon T_y)_y, \tag{4.2}$$

where we specify the following boundary conditions

$$\begin{aligned} \text{North:} \quad & T + \epsilon\frac{\partial T}{\partial n} &&= T_\infty \\ \text{South:} \quad & \frac{\partial T}{\partial n} &&= 0 \\ \text{East:} \quad & \frac{\partial T}{\partial n} &&= 0 \\ \text{West:} \quad & \bar{u}T - \epsilon\frac{\partial T}{\partial n} &&= 5\bar{u}\sqrt{\epsilon}(1 - e^{-\alpha y}). \end{aligned} \tag{4.3}$$

In Eq. (4.2), T is the temperature distribution, $(\bar{u}, \bar{v})$ the velocity field, ϵ the viscosity. The velocity field $(\bar{u}, \bar{v})$ is divergence free and can be considered as coming from an incompressible Navier–Stokes solution. The boundary conditions in Eq. (4.3) are a subset of the general ones derived previously. To simulate a boundary layer, the quantities $\bar{u}, \bar{v}$ and ϵ are chosen as

$$(\bar{u}, \bar{v}) = \left(1 - e^{-\alpha y}, 0\right), \qquad \epsilon = 0.01, \qquad \alpha = 1/\sqrt{\epsilon}, \tag{4.4}$$

where $T_\infty = 5\sqrt{\epsilon}$ and $\dfrac{\partial T}{\partial n} = n \cdot \nabla T$. The velocity field is generated on the unit square, then injected on the corresponding grid points of the varying domain. The simplified velocity field in Eq. (4.4) satisfies the divergence relation, and has a boundary layer.

4.3. *Statistical results*

In the calculations below, the 4th-order Runge-Kutta method is used together with 3rd-order SBP-operators on a grid with 50 grid points in both space directions and 9000 grid points in time, in order to minimize the time discretization error. In the uncertainty quantification analysis we have used 20 grid points in both the θ_1- and θ_2-directions.

We start by enforcing the following stochastic variation on the south boundary of the geometry (see Figure 2)

$$y_S(x, \theta_1, \theta_2) = 0.05\theta_1 \sin(2\pi x\theta_2),$$

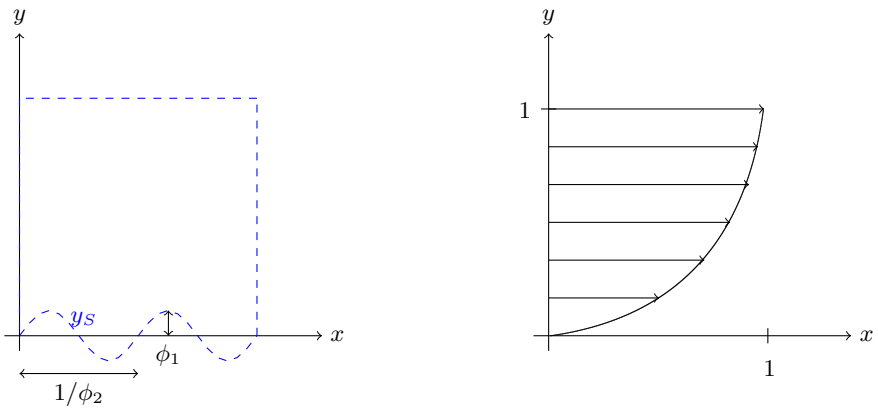

FIGURE 2: A schematic of the computational domain with definitions of y_S, θ_1 and θ_2 is shown to the left. The velocity profile for $(\bar{u}, \bar{v})$ as a function of y is shown to the right.

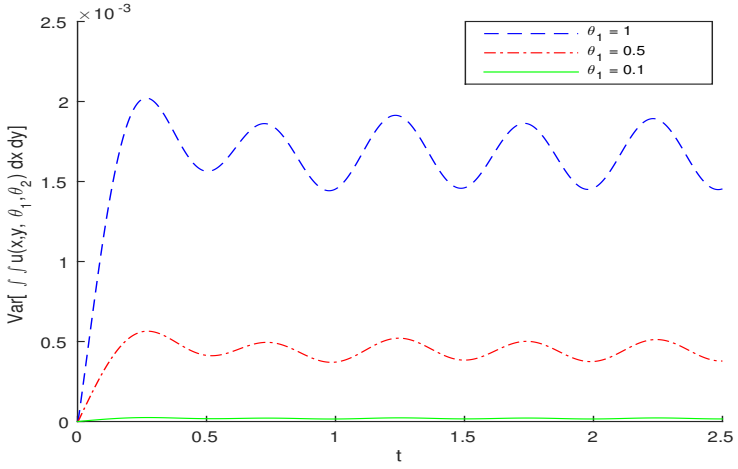

FIGURE 3: The variance of the linear functional $\iint_\Omega u(x, y, t, \theta)\, dx\, dy$ with respect to θ_2 (frequency) for different realizations of θ_1 (amplitude).

where $\theta_1 \sim N(-1, 1)$ and $\theta_2 \sim U(2, 10)$ are stochastic variables controlling the amplitude and frequency of the periodic variation, respectively.

As typical measures of the results, we compute statistics of the integral of the solution over the domain, that is

$$\iint_\Omega u(x, y, t, \theta_1, \theta_2)\, dx\, dy,$$

Figure 3 shows the variance with respect to θ_2 of the integral of the solution as a function of time for different realizations of θ_1. Figure 3 illustrates the fact that the variance increases with increasing amplitude. Hence, high-amplitude randomness in the geometry affects the solution more than low-amplitude randomness, as could be expected.

Figure 4 shows the variance with respect to θ_1 of the integral of the solution as a function of time for fixed values of θ_2. As can be seen, there is a trend towards increased

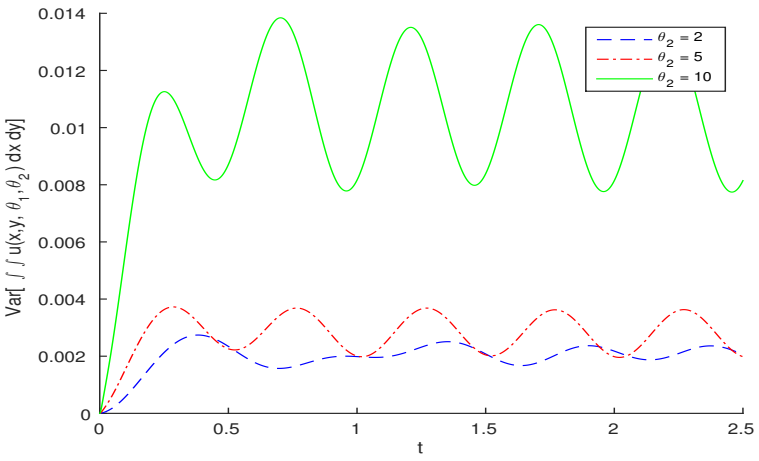

FIGURE 4: The variance of the linear functional $\int\int_\Omega u(x, y, t, \theta)\, dx\, dy$ with respect to θ_1 (amplitude) for different realizations of θ_2 (frequency).

variance for an increased frequency. Hence high-frequency random variation in the geometry affects the solution more than low-frequency random variation. However, since the variance of the cases $\theta_2 = 2$ and $\theta_2 = 5$ are of similar magnitude, a crystal clear conclusion cannot be drawn.

5. Conclusions and future work

We have studied how the solution to the advection–diffusion equation is affected by imposing boundary data on a stochastically varying geometry. The problem was transformed to the unit square, resulting in a formulation with stochastically varying wave speeds. Strong well-posedness and strong stability were proven.

The variances were computed for different fixed realizations of θ_1 (when varying θ_2) and θ_2 (when varying θ_1) controlling the amplitude and frequency, respectively. A tentative conclusion is that an increased frequency of the randomness in the geometry leads to an increased variance in the solution. Also, as expected, the variance of the solution grows as the amplitude of the randomness in the geometry increases.

REFERENCES

ANTOHE, B. & LAGE, J. 1997 A general two-equation macroscopic turbulence model for incompressible flow in porous media. *Int. J. Heat Mass Tran.* **40**, 3013–3024.

ELIASSON, P., ERIKSSON, S. & NORDSTRÖM, J. 2009 The influence of weak and strong solid wall boundary conditions on the convergence to steady-state of the navier-stokes equations. *AIAA Paper* 2009-3551.

FARHAT, C., GEUZAINE, P. & GRANDMONT, C. 2001 The discrete geometric conservation law and the nonlinear stability of ALE schemes for the solution of flow problems on moving grids. *J. Comput. Phys.* **174**, 669–694.

LIN, G., SU, C.-H. & KARNIADAKIS, G. E. 2008 Stochastic modeling of random rough-

ness in shock scattering problems: theory and simulations. *Comput. Method Appl. M.* **197** , 3420–3434.

Lin, G., Tartakovsky, A. M. & Tartakovsky, D. M. 2010 Uncertainty quantification via random domain decomposition and probabilistic collocation on sparse grids. *J. Comput. Phys.* **229**, 6995–7012.

Mendes, M. A. A., Ray, S., Pereira, J. M. C., Pereira, J. C. F. & Trimis, D. 2012 Quantification of uncertainty propagation due to input parameters for simple heat transfer problems. *Int. J. Therm. Sci.* **60**, 94–105.

Nordström, J. 2006 Conservative finite difference formulations, variable coefficients, energy estimates and artificial dissipation. *J. Sci. Comput.* **29**, 375–404.

Nordström, J., Eriksson, S. & Eliasson, P. 2012 Weak and strong wall boundary procedures and convergence to steady-state of the Navier–Stokes equations. *J. Comput. Phys.* **231**, 4867–4884.

Nordström, J. & Svärd, M. 2005 Well-posed boundary conditions for the Navier-Stokes equations. *SIAM J. Numer. Anal.* **43**, 1231–1255.

Nordström, J. & Wahlsten, M. 2015 Variance reduction through robust design of boundary conditions for stochastic hyperbolic systems of equations. *J. Comput. Phys.* **282**, 1–22.

Parussini, L., Pediroda, V. & Poloni, C. 2010 Prediction of geometric uncertainty effects on fluid dynamics by polynomial chaos and fictitious domain method. *Comput. & Fluids* **39**, 137–151.

Patankar, S. V. & Spalding, D. B. 1972 A calculation procedure for heat, mass and momentum transfer in three-dimensional parabolic flows. *Int. J. Heat Mass Tran.* **15**, 1787–1806.

Roache, P. J. 2002 Code verification by the method of manufactured solutions. *J. Fluid Eng.-Trans. ASME* **124**, 4–10.

Seban, R. A. 2012 Skin-friction and heat-transfer characteristics of a laminar boundary layer on a cylinder in axial incompressible flow. *J. Aeronaut. Sci.* **18**, 671–675.

Svärd, M. & Nordström, J. 2014*a* On the order of accuracy for difference approximations of initial-boundary value problems. *J. Comput. Phys.* **218**, 333–352.

Svärd, M. & Nordström, J. 2014*b* Review of summation-by-parts schemes for initial-boundary-value problems. *J. Comput. Phys.* **268**, 17–38.

Xiu, D. & Tartakovsky, D. M. 2006 Numerical methods for differential equations in random domains. *J. Sci. Comput.* **28**, 1167–1185.